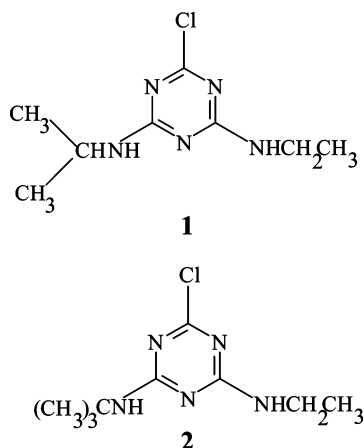


Surface Interactions of *s*-Triazine-Type Pesticides. An Electrochemical Impedance StudyMagdaléna Hromadová,[†] Romana Sokolová,[†] Lubomír Pospíšil,^{*,†} and Nicolangelo Fanelli[‡]*J. Heyrovsky Institute of Physical Chemistry, Academy of Sciences of the Czech Republic, Dolejškova 3, 18223 Prague, Istituto per i Processi Chimico-Fisici, Consiglio Nazionale delle Ricerche, via Moruzzi 1, 56124 Pisa, Italy**Received: October 12, 2005; In Final Form: January 9, 2006*

Two pesticides, atrazine and terbutylazine, have very similar chemical structures differing only by *iso*-propyl and *tert*-butyl substituents on their 6 amino groups. This minor structural difference causes profound effects in decomposition rates in the environment, leading to a ban of atrazine in the European Union. Here we present a study of adsorption at ideally polarized electrochemical interface in the absence of specifically adsorbed halides. The interfacial charge and the temperature determine which type of an adsorbed film is formed. The double layer capacitance measurements yield the critical temperature of the surface film transition, which is markedly different for the two pesticides. The time-resolved impedance spectroscopy indicates slow changes within the film structure that becomes disordered and can be characterized in terms of the fractal geometry.

Introduction

Pesticide compounds, which are the subject of this study, have a specific effect as plant growth regulators. Massive application of pesticides is motivated by promises of high-yields and high-quality food production. Symmetrical triazines (*s*-triazines)¹ are widely used for this purpose. Two representative derivatives are atrazine, **1**, (2-chloro-4-(ethylamino)-6-*tert*butylamino-1,3,5-triazine) and terbutylazine, **2**, (2-chloro-4-(ethylamino)-6-*tert*-butylamino-1,3,5-triazine). However, their application also



invokes an intensive concern of impacts on the environment and human health.² Reports indicate that, in the USA, more than 75 million pounds of atrazine are applied each year. Herbicidal activity³ of both compounds involves their binding to glutathione followed by inhibition of the electron-transfer chain in the photosystem II. The environmental decomposition is based on photolytic decomposition⁴ in the upper soil layers. Atrazine penetrates into groundwater, thus escaping photolysis, and it persistently contaminates sites where its application ceased

a long time ago. This finally led to the ban of atrazine by the European Commission, issued as decision no. 2004/248/EC. On the contrary, terbutylazine decomposes rapidly and formulations containing terbutylazine are considered safe for application. Very similar structures of **1** and **2** and, at the same time, a very different decomposition rate is an intriguing problem calling for identification of subtle nuances responsible for these undesirable effects. A shorter residence time of **1** in light-exposed soil layers could be caused by a different adsorbability on solid particles or other heterogeneous interfaces.^{5,6} Distinction of adsorption properties of such similar compounds in the natural environment would be a difficult task. Hence, general features of their surface activity are best investigated on an ideally reproducible model interface. Since ions and charged micro-particles are part of the natural environment, it is convenient to assess the role of Coulombic interaction in an adsorption process using a heterogeneous interface, at which the electric charge is controlled in a precise way.⁷ A seemingly unrelated system, like the interface solution | electrode, still may yield some relevant features for adsorptivity in real systems.

Numerous N-heterocyclic compounds strongly adsorb at interfaces including the solution–electrode boundary. Electrochemical methods for investigation of adsorption processes offer an advantage to control the electric charge of the heterogeneous interface and to distinguish the role of adsorbate–adsorbate and Coulombic interactions. The change of adsorbate–surface interaction may lead to reorientation within the adsorbed layer. As an example, we recall that pyridine and 2,2'-bipyridine or their complexes and derivatives assume different surface orientation (perpendicular or parallel to the surface) according to the polarity of the electrode charge. The change of molecular orientation in an adsorbed layer is only one of several processes, which can take place at any interface. Strong adsorbate–adsorbate interaction often leads to a profound change of the adsorbed structure from a fluidlike film to a compact two-dimensional layer.⁸ Such a surface phase transition, or a new phase formation, is governed by nucleation-and-growth mechanism. Compact surface films are considerably more stable.

* Corresponding author: pospisil@jh-inst.cas.cz.

[†] Academy of Sciences of the Czech Republic.[‡] Consiglio Nazionale delle Ricerche.

Their desorption involves a process inverse to nuclei formation called the hole formation. Film phase transitions are characterized by a critical transient temperature T_c above which a condensed phase cannot be formed.⁹ Growth models leading to compact molecular films usually assume isotropic growth of a new phase at perimeters of nuclei. More complex compounds, which can mutually interact through several donor and acceptor sites, may not obey such simple model growth.¹⁰ Anisotropic growth results in new surface structures that are irregular and, hence, the value of the double layer capacity assumes different local values. It is known that an uneven capacity distribution leads to a frequency dispersion, which is often termed as the observation of a constant phase element (CPE) behavior.^{11,12} Ramified structures are best characterized in terms of the fractal dimension, which is related to the frequency dispersion and can be evaluated from CPE.

Adsorption and phase transitions of adsorbed films at charged metallic electrodes are conveniently investigated by a variety of electrochemical methods. Significant information is obtained from determination of the interfacial double layer capacitance as a function of the potential, adsorbate concentration, temperature and time elapsed from the instant of contact between the solution and the solid phase. In this work we applied the phase sensitive AC polarography for assessment of the range of potentials where the adsorption takes place. Sharp discontinuous change of the imaginary admittance component together with a hysteresis of AC polarograms indicates a phase transition of an adsorbed film. The time dependence of the double layer capacitance C allows distinction of the mass transfer and nucleation-controlled processes. The time-resolved impedance spectroscopy¹³ yields information on the scaling form of C from which the fractal dimension of the film can be deduced.

The present communication reports adsorption of **1** and **2** on an ideally polarizable, structureless, clean, and well reproducible interface of the mercury drop electrode in aqueous solutions of an electrolyte. The aim is to identify conditions for possible compact film formation, transient temperatures, and the evolution of the film compactness in time. Application of the methods mentioned above yielded differences in compact film formation of **1** and **2**.

Experimental Section

Atrazine and terbutylazine were purchased as a pesticides reference material from Dr. Ehrenstorfer, GmbH (Augsburg, Germany). Potassium fluoride and chloride were of analytical grade. Water was distilled and deionized by means of Millipore system. Electrochemical measurements were done using an electrochemical system for cyclic voltammetry, phase-sensitive AC polarography, and DC polarography. It consisted of a fast rise-time potentiostat, a lock-in amplifier (Stanford Research, model SRS830) and a frequency response analyzer (Stanford Research, model SRS760). The instruments were interfaced to a personal computer via an IEEE-interface card (PC-Lab, AdvanTech model PCL-848) and a data acquisition card (PCL-818) using 12-bit precision. Sine-wave frequency and amplitude for the phase-sensitive AC polarography and capacitance-time measurements were 320 Hz and 5 mV, respectively. Frequency dependence of the cell impedance was measured at an interval of 3–100 kHz. The number of measured data points, number of settling cycles, and integration cycles was selected in such a way that the measurement time is negligible in respect to the time change of the interfacial capacitance and at the same time the noise/signal ratio is low. A three-electrode electrochemical cell was thermostated using Ministat CC (Huber, Germany).

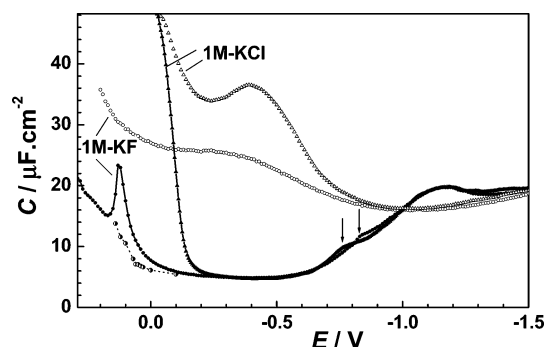


Figure 1. The double layer capacity of aqueous 1 M KCl (triangles) and 1 M KF (circles) in the absence (empty points) and in the presence of 0.2 mM atrazine (full points). The half-full round points show values from $C-t$ curves at time 10 s. Two arrows indicate a discontinuity. Data were measured at a frequency of 320 Hz.

The reference electrode, Ag|AgCl|1M LiCl, was separated from the test solution by a salt bridge. The working electrode was a valve-operated static mercury electrode (SMDE2, Laboratorní Přístroje, Prague) with an area 1.13×10^{-2} cm² and a mechanically controlled drop time. The auxiliary electrode was cylindrical platinum net. Oxygen was removed from the solution by a passing stream of argon.

Results and Discussion

Both *s*-triazines **1** and **2** are redox active only in their protonated forms¹⁴ and at rather negative potentials. Here we used purposely neutral aqueous solutions, in which no faradaic processes are observed. Strong adsorption of **1** is evidenced on the shape of the imaginary admittance component $Y'' \sim \omega C$, where C is the double layer capacity and ω is the perturbation frequency. Figure 1 shows a considerable decrease of C in two electrolytes, potassium chloride and potassium fluoride, in the presence of an equal concentration of **1**. The capacitance depression begins for both electrolytes in the same range of negative potentials. There are substantial differences at higher potentials. In the presence of chlorides, the capacity lowering ceases at -0.1 V, whereas in fluoride solution, it appears at a sharp maximum at $+0.1$ V, and the double layer capacity at all positive potentials remains much lower than in the blank. The capacitance-potential curves ($C-E$ curves) show still one faint feature near -0.8 V (marked by arrows). We will show later that a small break marks a potential E_L at which adsorbed layer condensation has its boundary. At positive potentials, chloride anions are specifically adsorbed at mercury electrodes, whereas fluoride is one of few ions that does not adsorb specifically at all.¹⁵ The preferential specific adsorption of chloride anions prevents the adsorption of **1**, which explains why **1** desorbs at the highest potentials so differently in both media. For this reason further experiments were performed only in the presence of potassium fluoride. AC polarograms measured on a stationary mercury drop electrode show hysteresis of desorption edge at -0.1 V in chlorides and a peak at $+0.1$ V in fluoride.

The shape and height of a sharp admittance peak at $+0.1$ V depends on the DC voltage scan rate and also on the scan direction. Since, on both sides of this peak, the C values are much lower than in the blank, this peak cannot correspond to a desorption maximum.¹⁶ It is likely that the rate process yielding this peak is due to the reorientation of adsorbate molecules. Experiments using a slow voltage scan yielded results depending, also, on the starting potential and the accumulation time, generally they were difficult to interpret and they were discontinued. Better insight to a time evolution of the surface

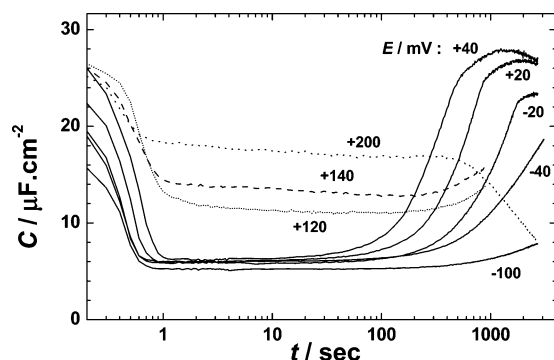


Figure 2. The time dependence of the double layer capacity of aqueous 0.2 mM atrazine in 1 M KF at constant applied DC potentials is indicated at each curve. The time scale is derived from an instant of the computer-triggered formation of a new mercury drop electrode.

layer is offered by long-time measurements of the double layer capacitance (C - t curves) at a constant DC potential. A selected set of C - t curves at potentials from -0.1 V to $+0.2$ V (the potential range of a sharp "reorientation" peak) is shown in Figure 2. These measurements are technically rather difficult because they require a good stability of the hanging mercury drop electrode over a period of almost an hour. Any imperfections at the capillary orifice and also mechanical vibration may cause a loss of contact or a fall of the mercury drop. Data in Figure 2 imply that the sharp peak at $+0.1$ V in Figure 1 would not be observed if the electrode surface were exposed to solution for a time from a few seconds to about 30 seconds. During that time period the C - t curves show constant values, which are also included in Figure 1 as half-full circles. The C - t curves clearly indicate that, at a given concentration and temperature, the adsorbed layer is rapidly established within seconds or even less. However, the adsorbed layer at potentials near zero volts is metastable and evolves in time. At long time and at potentials from about -40 mV to $+40$ mV, a large increase of C is observed. Values of C pass through a maximum. The decay of C is seen; however, it is so slow that it was technically impossible to follow it to its final value. Nevertheless, the C - t curve obtained at $+0.200$ V seems to decay toward a final value equal to $6 \mu\text{F}\cdot\text{cm}^{-2}$, which is identical to one at negative potentials in the middle of the adsorption region. The time dependence of the structure of adsorbed layer of **1** just described leads to a requirement to measure the impedance (or AC polarograms) at identical conditions as far as the initial potential value and the voltage scan are concerned.

The observed sigmoidal shape of C - t curves at short time, hysteresis of AC polarograms, and a singularity on C - E curves at negative potentials indicate that, most likely, the adsorbed film of **1** undergoes a phase transition from an ordinary mobile two-dimensional structure to a more compact and rigid film, which resembles a molecular solid phase at the surface. This is an expected property, taking into account rather low solubility of **1**, which at the interface can cause a supersaturation. A sigmoidal shape of C - t transients reflects the dependence of the surface coverage on time. The surface coverage θ is related to the capacity of a bare surface C_0 , the capacity of a fully covered surface C_1 , and a capacity at a given instant $C(t)$ according to the parallel condenser model as

$$\theta = \frac{C_0 - C(t)}{C_0 - C_1} \quad (1)$$

In the case of a diffusion-controlled adsorption process θ and also $C(t)$ change with $t^{-1/2}$. This time dependence is,

evidently, not obeyed for the present system. A sigmoidal time dependence of $C(t)$ implies the existence of an induction period before the adsorbed structure begins to cover the surface. In most cases this type of adsorption kinetics can be described by Avrami-Canac model^{17,18} accounting for the nucleation-and-growth processes. This model yields the time dependence of θ in the form

$$\theta = 1 - \exp(-bt^m) \quad (2)$$

where b combines the overall nucleation-and-growth rates and m is related to the growth mechanism. The C - t transients at short time for all potentials shown in Figure 2 yield $m = 2$, which indicates an instantaneous nucleation process. The same values of m were found in solutions of potassium fluoride and in potassium chloride. Hence the nucleation process of **1** itself is not influenced by specific adsorption of chloride anions to an extent that the progressive rate of nuclei formation would gain the overall control.

The occurrence of the first order 2D phase transitions is caused by short-range attractive interaction between adsorbate molecules, which results in a cooperative process forming a supercritical size of nuclei. Surface molecular clusters of a certain minimum size (nuclei) then become growth centers of a new phase. External parameters, the bulk concentration, the temperature, and the electrode potential determine the energy of involved interactions (adsorbate-adsorbate, adsorbate-solvent, and solvent-solvent) and, hence, conditions for observing the phase transition.¹⁹⁻²¹ Numerous organic compounds undergo the film condensation, which causes a discontinuity on C - E curves at higher and lower potentials denoted as E_H and E_L , respectively. The difference $\Delta E = E_H - E_L$ is often called the width of a capacitance pit. Potentials at which discontinuities occur reflect the energy involved in condensation process and serve for determination of critical phase transition parameters. Models of the phase transition are often derived from the Ising lattice gas model for localized adsorption. Using a two-dimensional two-state Ising model, a relation was derived²²

$$(\Delta E)^2 = ART \ln c + BT + C \quad (3)$$

where c is the bulk concentration of the adsorbate and A , B , and C are constants. The quadratic dependence of the critical temperature on the width of the potential range ΔE where a compact film exists enables the estimation of the critical temperature at a given bulk concentration of adsorbing species.

The present system is characterized by a rather anomalous dependence of C on time, which leads to less sharp features on C - E curves. Singular points, instead of discontinuous steps, are observed at negative potentials (see arrows in Figure 1). The high-potential side of a "capacitance pit" is marked by a peak, which we tentatively assigned to a reorientation process, meaning that a condensed layer undergoes an inverse phase transition before the adsorbed molecules can take a different surface orientation. A low solubility of both compounds in water prevented us from performing a more complete analysis of concentration-temperature-potential profiles according to the eq 3. We limited our analysis to a constant concentration for both **1** and **2**. Hence, here the characteristic feature of electrochemical phase transitions will be the dependence of the potential range ΔE , where the compact film exists, on the temperature. The temperature dependence of C - E curves is shown in Figure 3 for **1** and in Figure 4 for **2**. Large differences in ΔE values for both *s*-triazines are obvious. Exact values of

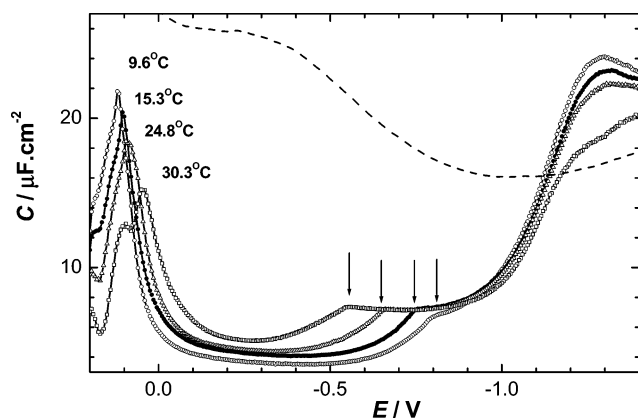


Figure 3. The double layer capacity of aqueous 1 M KF (dashed line) and in the presence of 0.2 mM atrazine (points) at temperature 9.6 °C (○), 15.3 °C (●), 24.8 °C (Δ), and 30.3 °C (□). Data were measured at a frequency of 320 Hz.

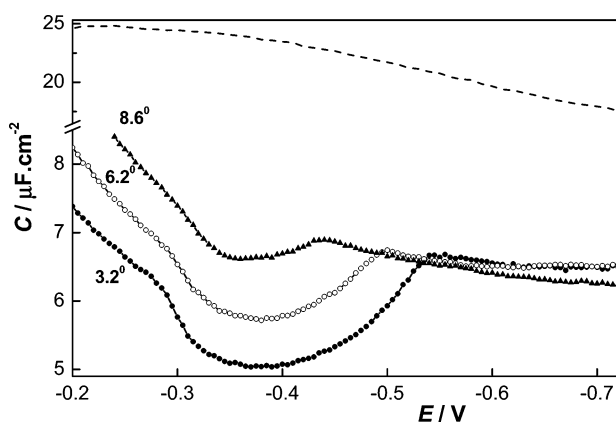


Figure 4. The double layer capacity of aqueous 1 M KF (dashed line) and in the presence of 0.2 mM terbutylazine (points) at temperature 3.2 °C (●), 6.2 °C (○), and 8.6 °C (▲). Data were measured at a frequency of 320 Hz.

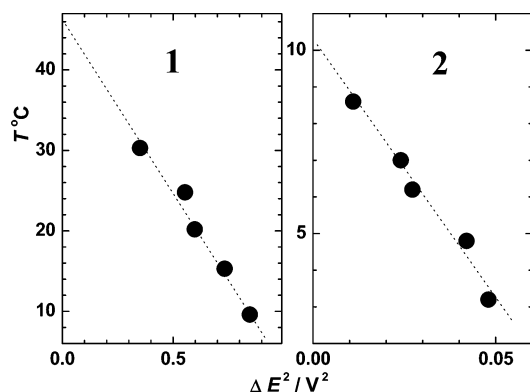


Figure 5. Determination of the critical temperature of the compact film formation for compounds **1** (left) and **2** (right) from the temperature dependence of the potential width of the capacitance pit at the bulk concentrations 0.2 mM. Estimated values of T_c are 46 °C for atrazine and 10.2 °C for terbutylazine.

E_H and E_L were obtained by a numerical differentiation of $C-E$ curves, and results are shown in Figure 5. Estimated values of the critical temperature at 0.2 mM concentrations are 46 °C for atrazine and 10.2 °C for terbutylazine. This remarkable difference for structurally similar compounds could be one of the reasons why they behave so differently in contamination of natural heterogeneous systems.

The anomalous shape of $C-t$ transients at long time deserves further attention (see Figure 2). The double layer capacity, which

changed with time according to eq 2 within 1–100 seconds, reached a very low value corresponding to the full coverage. Capacity increases again at longer time and passes through a maximum. This indicates that a seemingly final state of the full coverage at potentials of the pit edge is a metastable state. The increase of C is not a true desorption process because a second decay of C at the end of the observation time is clearly seen. The film rearrangement may involve a further phase separation, which changes a 2D structure into a 3D surface film. The long time effects can be also attributed to a reorientation process in which strongly interacting adsorbed molecules change their positions from a perpendicular to a parallel orientation toward the surface. Both hypothetical processes can cause a temporary decrease of θ and an interfacial inhomogeneity slowly evolving in time. At extremely long time, not accessible to experimental observation, the C values probably reach a low value again. A very slow decay of C after a maximum on $C-t$ curves suggests that small fractions of an adsorbate-free surface are not easily accessible for additional incorporation of molecules. Similar $C-t$ transients, showing a maximum at time of the order of hundreds or thousands of seconds, were observed for other adsorbing substances, however, such an effect was never seen for sulfur containing and strongly surface-attached adsorbates.

An interfacial inhomogeneity can be viewed as a surface roughness on a molecular scale. Randomized or repetitive roughness of electrode surfaces are frequently encountered at electrodes made of solid metals,¹² whereas the mercury drop electrode used in this study is an ideally smooth surface. Hence, any roughness, if confirmed, should be attributed only to the structure of an adsorbate. The problem of surface structures causing the frequency dependence of the electrode impedance is very general, and it was addressed in the past by many authors. In the absence of a redox reaction the electrode impedance Z of a structured surface behaves as^{11,23,24}

$$Z = R_s + \frac{1}{b(j\omega C)^\alpha} \quad (4)$$

where R_s is the resistance in series with the electrode capacitance, ω is the angular frequency, $j = \sqrt{-1}$, and b includes solution resistivity. The exponent α usually has values between 0.75 and 0.95. Equation 4 often describes the electrode impedance in a wide range of frequencies, which led us to denote α as the constant phase element. It was demonstrated that interfacial irregularities can be described in terms of the fractal geometry.²⁵ Numerous attempts were made to relate α to the Hausdorff fractal dimension D_H . The model of Nyikos–Pajkossy²⁴ uses a parallel combination of a large number of series RC circuits representing a given geometry of a purely capacitive admittance and yields:

$$\alpha = \frac{1}{D_H - 1} \quad (5)$$

Another model of a fractal interface uses Cantor bars or a Sierpinski gasket from which scaled transmission lines were derived yielding^{26,27}

$$\alpha = 3 - D_H \quad (6)$$

Our tentative explanation for a long-time capacitance maximum near the boundary potential of the compact layer considered a temporary restructuring of the adsorbed layer. This process could yield ramified patches of a compact film along with a bare surface, where further and very slow additional adsorption would

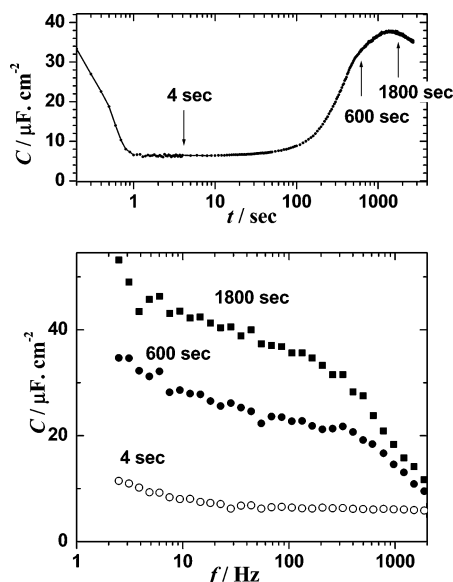


Figure 6. The double layer capacity of aqueous 0.2 mM atrazine in 1 M KF at the applied DC potential +0.040 V as a function of time (upper graph measured at 320 Hz) and as a function of the frequency of AC signal (lower graph). Arrows along the C - t curve indicate time at which three frequency spectra given in the lower graph were measured. The temperature was 20 °C. The amplitude of the superimposed AC voltage was 5 mV (p-p).

take place. In view of surface roughness theories^{28,29} it is plausible that such a temporary structure should yield the constant phase element behavior. Hence, we attempted to support or disprove the above-mentioned hypothesis by investigation of a possible frequency dispersion of C at different instants of the film growth. Typical results for a solution of **1** in 1M KF are shown in Figure 6. The C - t curve obtained at the potential +0.040 V is reproduced in Figure 6 and it is marked at times where the electrode impedance spectrum was measured. The double layer capacitance derived from the cell admittance as $C = Y/\omega$ is plotted for different time intervals elapsed from an instant of a fresh mercury drop formation. After 4 s the electrode surface is completely covered by a compact layer. At this time interval Y scales reasonably well with frequency, with an exponent $\alpha = 1$. Measurements of the impedance spectrum 600 or 1800 s after the mercury drop formation corresponds to a time where C - t maximum was observed. Those impedance spectra clearly indicate the presence of the "constant phase element" with an estimated value of $\alpha = 0.895$. Calculations using eq 5 or 6 yielded almost the identical value of the fractal dimension $D_H = 2.12$. Therefore, we refrain from any speculation about which of the two equations is more appropriate for the present case.

The development of the CPE behavior at long time supports the idea that the metastable film changes its structure to a three-dimensional, probably stacked film. This process is connected with a roughening of the interface on a molecular level, which leads to a detectable CPE. Figure 7 presents a similar set of data for solutions of **1** in 1M KCl. There it is shown that at a constant time of the film development the frequency dispersion of C is practically independent of the potential. The frequency spectrum in the absence of **1** or at potentials far from the pit edge yields constant frequency-independent C values, which proves that the observed frequency dispersion in other cases is not an artifact caused by an impurity or a stray instrumentation phase shift.

The present study indicates that even a minor structural change of a bio-active molecule may cause rather profound

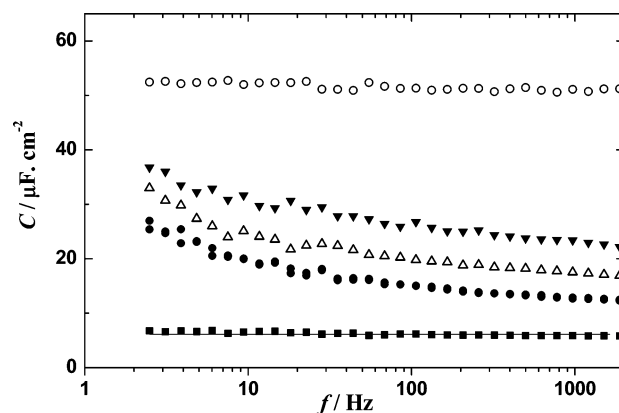


Figure 7. The double layer capacity of aqueous 0.2 mM atrazine in 1 M KCl as a function of the frequency of AC signal at different applied DC potentials: -0.122 V (\blacktriangledown), -0.128 V (Δ), -0.134 V (\bullet), and -0.200 V (\blacksquare). The frequency independence of the blank 1 M KCl at -0.100 V is given as the upper plot (\circ). The temperature was 20 °C. The amplitude of the superimposed AC voltage was 5 mV (p-p). Spectra were measured 300 s after a fresh mercury drop electrode was formed.

differences in accumulation properties at heterogeneous interfaces. Atrazine **1** and terbutylazine **2** differ just by one CH_3 group, which causes a dramatic change of their phase transition temperature. Higher T_c value of atrazine promotes the formation of the condensed adsorbed layer at all typical temperatures encountered in the environment. Considerably lower T_c of terbutylazine prevents its condensation, and it could be a reason this compound is more "environmentally friendly". Our study points to a certain possibility to predict environmental risks in newly introduced compounds by including the phase transition temperatures as a part of their important parameters.

Acknowledgment. This work was supported by the Grant Agency of the Czech Republic 203/03/0821, Grant Agency of the Academy of Sciences of the Czech Rep. A400400505 and Ministry of Education of the Czech Republic LC510. Joint cooperation was made possible on basis of the cooperation agreement between C.N.R. Rome and the Academy of Sciences of the Czech Republic.

References and Notes

- (1) Worthing, C. R.; Phil, D. *The Pesticide Manual*; British Crop Protection Council: Hampshire, UK, 1987.
- (2) Hamernik, K. *Pure Appl. Chem.* **2003**, *75*, 2531.
- (3) Draber, V. W.; Kluth, J. W.; Tietjen, K.; Trebst, A. *Angew. Chem.* **1991**, *103*, 1650.
- (4) Lanyi, K.; Dinya, Z. *Microchem. J.* **2003**, *75*, 1.
- (5) Ulrich, P.; Weller, M. G.; Niessnes, R. *Fresenius J. Anal. Chem.* **1996**, *354*, 352.
- (6) Welhouse, G. J.; Barak, P.; Bleam, W. F. *J. Phys. Chem.* **1993**, *97*, 11589.
- (7) Sokolová, R.; Hromadová, M.; Pospíšil, L. *J. Electroanal. Chem.* **2003**, *552*, 53.
- (8) de Levie R. *Adv. Electrochem. Electrochem. Eng.*; J. Wiley: New York, 1986; p 1.
- (9) Pospíšil, L.; Emons, H.; Muller, E.; Dorfler, H. *J. Electroanal. Chem.* **1984**, *170*, 319.
- (10) Pospíšil, L.; Zálšíš, S.; Sokolová, R.; Fanelli, N. *Acta Chim. Models in Chem.* **2000**, *137*, 383.
- (11) La Mehaute, A.; Crepy, G. *Solid State Ionics* **1983**, *9-10*, 275.
- (12) Mulder, W. H.; Sluyters, J. H. *Electrochim. Acta* **1988**, *33*, 301.
- (13) Pospíšil, L. *J. Phys. Chem.* **1988**, *92*, 2501.
- (14) Pospíšil, L.; Trsková, R.; Zálšíš, S.; Fuoco, R.; Colombini, M. P. *Microchem. J.* **1996**, *54*, 367.
- (15) Delahay, P. *Double Layer and Electrode Kinetics*; J. Wiley: New York, 1965.
- (16) Frumkin, A. N.; Melik-Gaykazian, V. I. *Dokl. Akad. Sci. SSSR* **1951**, *77*, 855.

- (17) Avrami, M. *J. Chem. Phys.* **1939**, 7, 1103.
- (18) Canac, F. *C. R. Acad. Sci.* **1933**, 196, 51.
- (19) Pushpalatha, K.; Sangaranarayanan, M. V. *J. Electroanal. Chem.* **1997**, 425, 39.
- (20) Retter, U. *J. Electroanal. Chem.* **1984**, 179, 25.
- (21) Retter, U. *Electrochim. Acta* **1996**, 41, 2171.
- (22) Shridharan, R.; de Levie, R.; Rangarayan, S. K. *Chem. Phys. Lett.* **1987**, 142, 43.
- (23) De Levie, R. *J. Electroanal. Chem.* **1990**, 281, 1.
- (24) Nyikos, L.; Pajkossy, T. *Electrochim. Acta* **1985**, 30, 1533.
- (25) Avnir, D.; Farin, D.; Pfeifer, P. *New J. Chem.* **1992**, 16, 439.
- (26) Liu, S. H. *Phys. Rev. Lett.* **1985**, 55, 529.
- (27) Sapoval, B. *Solid State Ionics* **1987**, 23, 253.
- (28) Farin D.; Avnir, D. Chapter 4.12. *The Fractal Approach to Heterogeneous Chemistry*; J. Wiley: New York, 1989; pp 271–293.
- (29) Meakin, P. *CRC Critical Reviews in Solid State and Material Science* **1987**, 13, 143.